



Observational studies of mean radiant temperature across different outdoor spaces under shaded conditions in densely built environment



Alan Lai ^{a, *}, Minjung Maing ^{a, 1}, Edward Ng ^{a, b, c}

^a School of Architecture, The Chinese University of Hong Kong, Shatin, Hong Kong, China

^b Institute of Future Cities, The Chinese University of Hong Kong, Shatin, Hong Kong, China

^c Institute of Environment, Energy and Sustainability, The Chinese University of Hong Kong, Shatin, Hong Kong, China

ARTICLE INFO

Article history:

Received 14 October 2016

Received in revised form

28 November 2016

Accepted 25 December 2016

Available online 27 December 2016

Keywords:

Mean radiant temperature (MRT)

Long-wave mean radiant temperature (LMRT)

Horizontal radiant fluxes

Horizontal Sky View Factor (HSVF)

Sky View Factor (SVF)

ABSTRACT

High-density urban environment affects urban microclimate, and thermal comfort of outdoor spaces. Shading by urban structure is the primary measure to reduce daytime mean radiant temperature (MRT) by blocking direct solar radiation. However, it is believed that overly-restricted Sky View Factor (SVF) limits the radiative cooling by the sky of lower effective temperature. Therefore, this study aimed at examining the relationship between SVF and MRT in built environment. To investigate the dependence of MRT on SVF via radiant fluxes, this study performed field measurement of six directional long-wave, short-wave fluxes and MRT across a number of outdoor spaces under shaded in densely built environment. Regression analysis was employed in examining desired relationships. Across different open spaces, MRT would increase by 1.6 K per 10 W/m² increase of either long-wave or short-wave radiant fluxes. Global solar radiation and air temperature are the most influential meteorological parameters affecting radiant fluxes components in MRT. Besides, this study suggests the use of long-wave mean radiant temperature (LMRT) representing effective surface temperature of surrounding objects. LMRT generally follows the temporal pattern of reference air temperature. In a case study, if SVF is decreased by 0.1, the weighted sum of long-wave fluxes would be increased by 10 W/m². This would bring an increase of 1.6 K in MRT. But, SVF has weak explanatory power to variations in short-wave fluxes when under shaded. Larger SVF is preferred for cooling open space in hot and humid region if direct sunlight is already blocked by urban morphology.

© 2016 Elsevier Ltd. All rights reserved.

1. Introduction

The design of outdoor thermal comfortable space has increasingly been the object of study in recent years. A thermally comfort outdoor space encourages people to utilize it [1,2]. And people will get healthier with increased outdoor activity [3,4]. Therefore, it is crucial to design comfortable open spaces for people to live healthily in the densely built environment.

To assess objectively the thermal comfort level of a space (either indoor or outdoor), a number of thermal indices are commonly employed with measurement of four fundamental physical parameters: air temperature, relative humidity, air velocity, and mean

radiant temperature [5–7]. Mean radiant temperature, MRT, is a quantity linking the radiant energy transfer between a human body and the surrounding to which the body exposed [8]. With radiation energy fluxes of all possible directions and wavelengths due to the (built) environment, MRT is significantly dependent on the sum of long-wave and short-wave radiant energy fluxes approaching to a human body [4]. Because it is closely related to the human energy balance, MRT is one of the important parameters in the widely used thermal assessment, for example, Physiological Equivalent Temperature PET [9], and Universal Thermal Climate Index (UTCI) [10]. Moreover, without the direct short-wave from the sun, the fluctuation in MRT is diminished at night time outdoor [4]; MRT is even degenerated to the air temperature T_a of a room in daytime with negligible amount of direct solar radiation as the radiant fluxes and surface temperatures are uniform within the indoor space [11]. These empirical results are consistent with the assumed equivalence between MRT and air temperature under negligible sunlight conditions like either indoor daytime, or outdoor night time

* Corresponding author.

E-mail addresses: alan.laiki@gmail.com (A. Lai), maing@hku.hk (M. Maing), edwardng@cuhk.edu.hk (E. Ng).

¹ Present Address: Faculty of Architecture, The University of Hong Kong, Hong Kong, China.

Nomenclature

Symbols and acronyms

ASHRAE	American Society of Heating, Refrigerating and Air-Conditioning Engineers
HSVF	Horizontal Sky View Factor
K	Short-wave fluxes with wavelength between 300 and 2800 nm
K_{Downward}	Downward short-wave fluxes
K_{Easterly}	Easterly short-wave fluxes
$K_{\text{Northerly}}$	Northerly short-wave fluxes
$K_{\text{Southerly}}$	Southerly short-wave fluxes
K_{Westerly}	Westerly short-wave fluxes
LMRT	Long-wave Mean Radiant Temperature
L	Long-wave fluxes with wavelength between 4.5 and 42 μm
L_{Downward}	Downward long-wave fluxes
L_{Easterly}	Easterly long-wave fluxes
$L_{\text{Northerly}}$	Northerly long-wave fluxes

$L_{\text{Southerly}}$	Southerly long-wave fluxes
L_{Westerly}	Westerly long-wave fluxes
MRT	Mean Radiant Temperature
PET	Physiological Equivalent Temperature
RMSE	Root mean square error
SVF	Sky View Factor
SVF_{Downward}	The conventional Sky View Factor was taken with the fisheye lens facing upward to capture downward photons of visible light
SVF_{Easterly}	SVF was taken with fisheye lens facing the east to capture easterly photons of visible light
$SVF_{\text{Northerly}}$	SVF was taken with fisheye lens facing the north to capture northerly photons of visible light
$SVF_{\text{Southerly}}$	SVF was taken with fisheye lens facing the south to capture southerly photons of visible light
SVF_{Westerly}	SVF was taken with fisheye lens facing the west to capture westerly photons of visible light
UTCI	Universal Thermal Climate Index
WSumK	Weighted Sum of Short-wave fluxes
WSumL	Weighted Sum of Long-wave fluxes

[12–14]. Nonetheless, MRT is evidently one of the important parameters in assessing the thermal comfort of a space.

Numerous studies point out that shading, by buildings or trees, is important for providing daytime outdoor thermal comfort in an open space [2,4,15–23]. The level of shading by buildings is usually quantified by the following urban geometrical parameters: either the height-to-width ratio (H/W) for simple canyon geometry [2,17,20,22–24]; or the Sky View Factor (SVF) for complex urban structure [1,2,4,25]. A highly shaded environment can thus be created by increasing H/W of a simple street canyon [17,24,26]; or by lowering SVF of the built environment [4,18,21,27]. SVF is a dimensionless quantity ranging from zero to unity indicating the degree of obstruction from perspective of a single observation point in urban environment from totally obstructed to unobstructed [24]. In other words, lower values of SVF means more obstructed of an area; higher values of SVF indicates a more unobstructed area. The benefit of shading is mainly attributed to the blocking of direct short-wave radiant fluxes coming from the sun [1,4]. A significant lower values in MRT at sites are observed in the shade of more trees and buildings when compared with that at sites more exposed during daytime; in contrast to the night time, little difference in MRT between both sites are recorded in the absence of sunlight [4]. The main effect of shading is evident to the reduction in daytime MRT by blocking its direct short-wave component from the sun.

The shading effect of SVF on outdoor thermal comfort, especially on MRT, have been recently investigated in the past decade [1,4,18,19,28]. Regard to the relationship between SVF and MRT and its strength, several studies have shown higher SVF causes higher MRT under sunny conditions when exposed to beam solar radiation [4,19,28]. Tan (2013) [4] has reported there are simple positive correlations between SVF and MRT with coefficient of determination $R^2 = 0.61$ and 0.32 at two sites at 14:00 in Singapore. Lee (2014) [28] has also published the similar correlation R^2 is of 0.57 in southwest of Germany. Moreover, Lee [28] has introduced particularly the use of ‘southern part of upper half space (SVF_{90-270})’ rather than the traditional use of ‘whole upper half space’ where $SVF = SVF_{0-360}$. The correlation between SVF_{90-270} and MRT is 0.77 . This indicates that SVF_{90-270} is more correlated to MRT than traditional SVF (or SVF_{0-360}). It is because a higher proportion of overlapping between the sun path and southern part of sky view is in

the ‘southern part of upper half space (SVF_{90-270})’. Outdoor MRT is strongly affected by the direct short-wave fluxes from the sun in the southern part of upper half space. Besides, Krüger (2011) [19] has examined the correlation between SVF and the temperature difference ($\Delta\text{MRT-T}$), which is the difference between MRT and ambient temperature at reference station. This difference, ($\Delta\text{MRT-T}$) increases with larger SVF with coefficient of determination $R^2 = 0.57$. Krüger (2011) [19] has also attributed this correlation to the strong dependence of MRT on solar radiation. The findings of the above studies suggest that the short-wave component of MRT is largely attributed to the direct solar radiation from the sun in the unblocked sky, which under unshaded conditions. These seemingly indicate that the effect of SVF, either the whole SVF_{0-360} or the southern SVF_{90-270} , is mainly acting as an opening of an outdoor space for the direct short-wave fluxes from the sun. This is analogous to a large opening of a room exposed to the sun allowing more sunlight entering into the room.

Although a very high level of shading can block the direct solar radiation, overly restricted sky view also limit the radiative loss from the built environment resulting in more solar heat absorption [29]. The resulting densely built environment may cause the retention of the radiant fluxes, especially the long-wave one [29]. A higher level of shading (less sky view) causes more absorption of long-wave fluxes by the deeper canyon [29]. Higher SVF decreases the sum of long-wave fluxes from surrounding [27]. Tan (2013) [4] also points out that, among the six directional fluxes, the downward long-wave radiation is noticeably the least one due to facing more sky view but not terrestrial surface. Because the effective temperature of the sky is much lower than the terrestrial surfaces [30]. Each horizontal radiant fluxes is also important for the MRT [27]. The difference in MRT is attributed to the variations in the six directional radiant fluxes due to densely built environment [4,31]. It should be noted, however, that there have been very few attempts to establish a direct relationship between Sky View Factor and daytime downward and horizontal radiant fluxes, especially long-wave fluxes.

While considerable attention has been paid to the shading effect of urban morphology for reducing the MRT at the first place by blocking its direct short-wave radiant fluxes from the sun, little empirical research have been reported on how urban morphology

influence daytime MRT in detail through the individual long-wave and short-wave radiant fluxes in the open space, when under shaded conditions, in order to further improve the outdoor thermal comfort. This lead to a question, to what extent, the effect of urban morphology, represented by SVF, is optimal for outdoor thermal comfort of an open space?

The major purpose of this paper is therefore to deepen our physical understanding of how urban morphology affect mean radiant temperature via its component radiant fluxes, either short-wave or long-wave fluxes, under shaded conditions. The mean radiant temperature MRT depends on both short-wave and long-wave radiant fluxes. This study firstly examined, to what degree, how the MRT depends on its long-wave and short-wave components across different open spaces and different climatic conditions; and in turn, more importantly, how the downward and horizontal radiant fluxes correlated to urban morphology under given climatic conditions of global solar radiation, and air temperature. Therefore, this study investigate the following relationships:

1. Dependence of MRT on long-wave, and short-wave radiant fluxes;
2. Dependence of MRT, its long-wave and short-wave components on climatic conditions: reference air temperature, and global solar radiation;
3. Dependence of directional long-wave, and short-wave radiant fluxes on urban morphology under given climatic conditions;

2. Methodology

2.1. Mean radiant temperature MRT

The mean radiant temperature, T_{mrt} or MRT, which can be regarded as a weighted sum of all long- and short-wave radiant fluxes (including direct, reflected and diffuse components), to which a human body is exposed, is one of the most important meteorological parameters related to human energy balance and human thermal comfort. By definition, MRT is the 'uniform temperature of an imaginary enclosure in which the radiant heat transfer in the actual non-uniform enclosure' [8].

Mean radiant temperature can be obtained by *integral radiation measurements*. This method is the most accurate one to estimate outdoor MRT [32]. To evaluate MRT, the mean radiant flux density S_{str} of a human body is firstly calculated by multiplying the six individual measurements of the short-wave and long-wave radiant fluxes with the corresponding weights, namely the view factors F_i ($i = 1-6$) between a person and the surrounding surfaces according to Equation (1) [33]:

$$S_{str} = \alpha_k \sum_{i=1}^6 F_i K_i + \epsilon_p \sum_{i=1}^6 F_i L_i, \quad i = [1, 6] \quad (1)$$

K_i = the short-wave radiant fluxes from the i -th direction

L_i = the long-wave radiant fluxes from the i -th direction

F_i = the view factors between a person and surrounding surfaces

α_k = the absorption coefficient for short-wave fluxes (standard value 0.7)

ϵ_p = the emissivity of human body. According to Krichhoff's laws ϵ_p is equal to the absorption coefficient for long-wave radiation (standard value 0.97)

The angular factor (or view factor), F_i , is determined by both position and orientation of a person [5]. To put it simply, for a (rotationally symmetric) standing or walking person F_i is set to 0.22 for radiant fluxes from the four cardinal directions (Northerly, Easterly, Southerly, and Westerly) and 0.06 for radiant fluxes from sky and the ground, respectively. For a sphere, F_i is set to be one-sixth (i.e. $1/6 \approx 0.167$) for all six directions. In this study, by specifying the values of F_i for a rotationally symmetric standing or walking person, the mean radiant flux density S_{str} is calculated and thus the MRT ($^{\circ}\text{C}$) is obtained from Stefan-Boltzmann law:

$$MRT = (S_{str}/\epsilon_p\sigma)^{0.25} - 273.15 \quad (2)$$

σ = the Stefan-Boltzmann constant ($5.67 \times 10^{-8} \text{ Wm}^{-2}\text{K}^{-4}$)

2.2. Weighted sum of directional radiant fluxes

The six individual measurements of long-wave radiant fluxes were added to a sum, W. Sum L, with corresponding weight taking into account of both angular factor and emissivity of human body according to equation (3). Similarly, with corresponding weight of both angular factor and absorption coefficient for short-wave fluxes, the equation of W. Sum K is given by equation (4).

$$W.SumL = \epsilon_p \sum_{i=1}^6 F_i L_i \quad (3)$$

$$W.SumK = \alpha_k \sum_{i=1}^6 F_i K_i \quad (4)$$

2.3. Long-wave mean radiant temperature LMRT

This study proposes the use of Long-wave Mean Radiant Temperature (LMRT). By substituting $S_{str} = W.SumL$ into equation (2), LMRT is the degenerated MRT taking only accounts of long-wave radiant fluxes. It should represent the effective mean surface temperature of surrounding objects in urban environment under given climatic conditions of given global solar radiation, and air temperature. It is believed that LMRT is correlated to the ambient air temperature. This is one of the relationships to be examined in this study.

2.4. Instrumentations for directional radiant fluxes and MRT

The three dimensional long-wave and short-wave radiant fluxes were recorded by the net radiometers (Kipp & Zonen, CNR4) [34]. The three CNR4 net radiometers were mounted on a tripod (see Fig. 1) for measuring long-wave and short-wave radiant fluxes from the six directions namely, the sky dome (Downward fluxes), the ground (Upward fluxes), and the four horizontal directions (Northerly, Easterly, Southerly and Westerly). Measurements were conducted at a height of around 1.5 m above ground level. The net radiometers were recently calibrated by the manufacturer.

Measurements were taken from 15:00 to 16:00 on each day. Since the objective of this study is to investigate the effect of urban morphology on radiant fluxes and in turn on the mean radiant temperature under shaded so as to deepen the scientific understanding of how open spaces should be designed for better outdoor thermal comfort allowing local residents to enjoy and live in a



Fig. 1. An experimental setup of three Net Radiometer CNR4 in an open space for measuring three dimensional radiant fluxes from the six directions.

healthier environment. Measurements were therefore chosen in the hottest period between 15:00 and 16:00 on each day, and, at the same time, the beam solar radiation from high angle sun in the early afternoon could also be prevented from overwhelming the effect of urban morphology on radiant fluxes. The daily mean air temperature of Hong Kong normally reaches its maximum starting from around 13:00 and starts to drop around 16:00 in Hong Kong summer. Also, the sun is at its highest angle, which is nearly normal to the ground in the summer of Hong Kong, between the period 12:30 and 13:00. The effect of beam solar radiation on the sensors would thus overwhelm the effect of urban morphology on radiant fluxes. Besides, local residents therefore usually start to increase their outdoor activities from around 15:00 in summer of Hong Kong. As a result, the time slot between 15:00 and 16:00 was chosen to study the effect of urban morphology on radiant fluxes, and in turn on the mean radiant temperature as outdoor thermal comfort index in this study. The logging interval was set as 10 s and the measured radiant fluxes were smoothed out using 5-min mean value. For simplicity, this study extracts only 5-min mean values at 15:00, 15:15, 15:30, and 15:45. Time of measurement when sensors recording direct sunlight would be eliminated for regression analysis so as to examine the radiant fluxes under shaded.

2.5. Area of study

The first aim of the study is focusing on how the MRT depends on its long-wave and short-wave components under shaded across different open spaces and different climatic conditions, namely air temperature and global solar radiation in different months. The field study was conducted in Hong Kong from June to November 2015 in six different open spaces as Fig. 2: A) between residential and commercial buildings on June 4, 2015; B) an open podium in a university campus with adjacent short, loosely packed student hostels on September 15, 2015; C) a courtyard enclosed by a C-shaped student hostel building on September 25, 2015; D) in another commercial area surrounded by a number of curtain wall buildings on October 16, 2015; E) a podium in an university campus enclosed by tall buildings of teaching and office; on November 18, 2015; F) a podium surrounded by public housing buildings within a public estate on November 19, 2015. The experiment were performed on fair clear sky days. This field study covered a wide range of climatic conditions and open spaces appear in Hong Kong. The

testing points in the open spaces depended on the 1) availability of equipment on the days of measurement; 2) availability of permitted spaces, and; 3) no beam solar radiation incident on the net radiometers. A total of 15 testing points were measured as in Table 1.

2.6. Background climatic conditions on days of measurement

The reference air temperature, T_o , taken from the headquarter of Hong Kong Observatory (HKOC) Manned Weather Station ($22^{\circ}18'07''N$, $114^{\circ}10'27''E$) which is located at roughly the centre of Hong Kong, was used to be the representative air temperature of Hong Kong on the days of measurement in this study.

On the other hand, the global solar radiation K_g were extracted from the Kau Sai Chau (KSC) Automatic Weather Station ($22^{\circ}22'13''N$, $114^{\circ}18'45''E$) of Hong Kong Observatory. The distance between the two stations HKOC and KSC is around 16 km. In fact, the global solar radiation K_g in Hong Kong were recorded independently by only two weather stations of Hong Kong Observatory: one is at Kau Sai Chau, KSC, ($22^{\circ}22'13''N$, $114^{\circ}18'45''E$), and another is at King's Park, KP, ($22^{\circ}18'43''N$, $114^{\circ}10'22''E$). However, there were missing data of global solar radiation from weather station at King's Park due to equipment problems on several days of measurement in this study. Therefore, the data of global solar radiation were only extracted from station KSC.

3. Results and discussion

This study aims at investigating, within open spaces, the dependence of MRT on both long-wave and short-wave radiant fluxes, its dependence on climatic conditions, dependence of radiant fluxes on climatic conditions and urban morphology, and the relationship between MRT and SVF. The physical parameters and thermal index deployed in this study were long-wave, short-wave radiant fluxes, and mean radiant temperature MRT. Single-point field measurement of long-wave, short-wave radiant fluxes and MRT across 6 different outdoor spaces were performed mostly in the summer 2015 during afternoon 15:00–16:00 as the afternoon session is generally the hottest period of a day in Hong Kong.

3.1. Correlation between the thermal indices MRT and LMRT

To examine the dependence of MRT on radiant fluxes, this study proposes the use of long-wave mean radiant temperature LMRT, which is the MRT taking accounts of only long-wave radiant fluxes. Therefore, the thermal index, mean radiant temperature MRT is decomposed respectively into its long-wave and short-wave components: long-wave mean radiant temperature LMRT; and the residual part, the difference between MRT and LMRT (MRT-LMRT).

This study first investigates the correlation between MRT and LMRT as shown in Fig. 3a. These two parameters are positively and highly associated with the coefficient of determination $R^2 = 0.78$. The higher LMRT, the higher surface temperatures of ambient environment, and higher the mean radiant temperature that a person experiences in shaded outdoor area. But, the correlation between MRT and (MRT-LMRT), representing the effect of short-wave radiant fluxes, is low ($R^2 = 0.60$). The results suggest that the effective surface temperature of surrounding has a higher explanatory power for the outdoor MRT under shaded area as LMRT is highly associated with MRT.

3.2. Correlation between MRT and radiant fluxes

This session examine the correlation between LMRT and weighted sum of long-wave fluxes WSumL ($R^2 = 0.9999$) as shown in Fig. 4a; and that between (MRT-LMRT) and weighted sum of

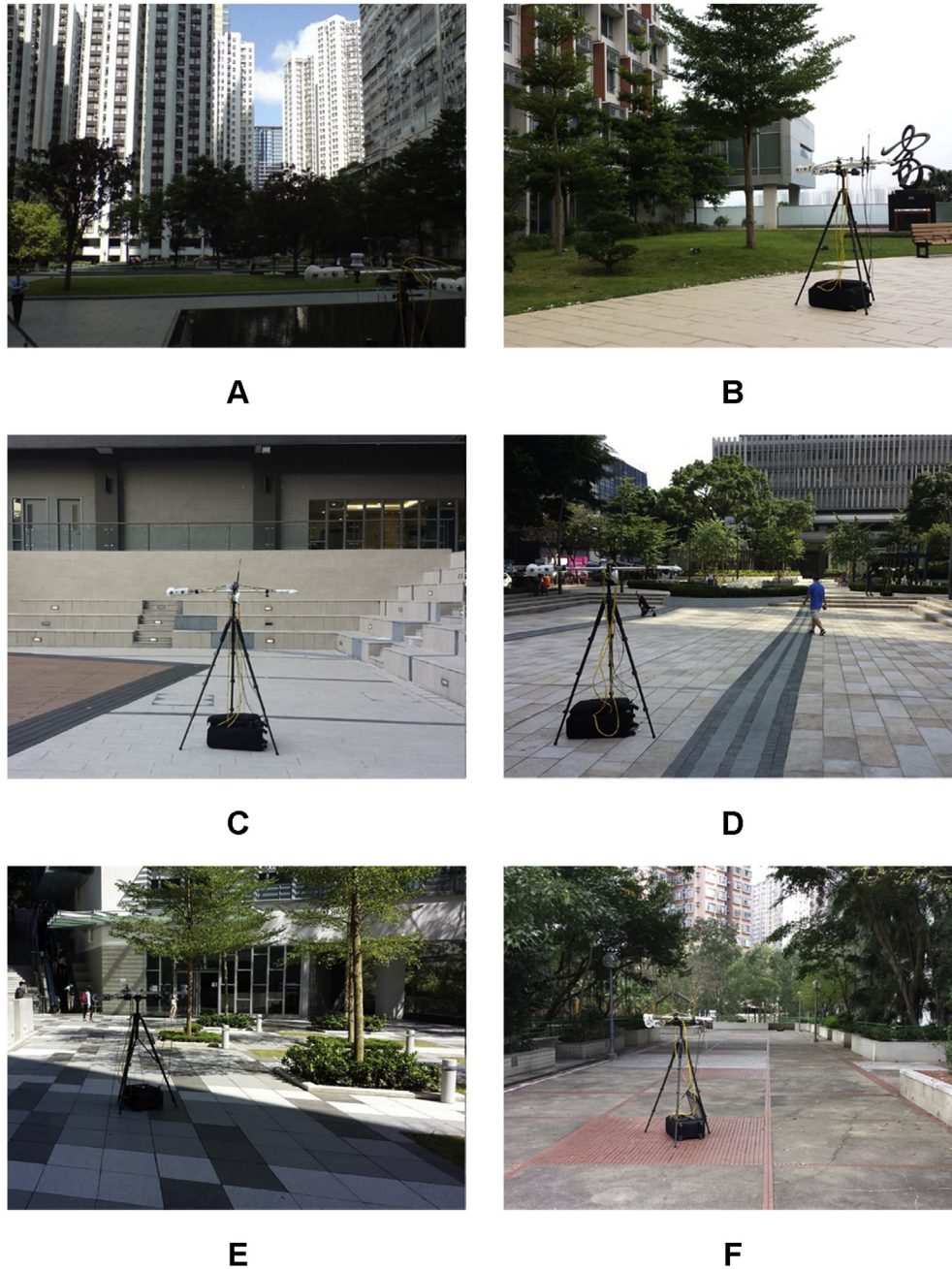


Fig. 2. Sites photos for the 6 different open spaces.

Table 1
Description of measurement points.

Area	Description of open spaces	No. of Points	Date
A	Open space between residential and commercial buildings	A1, A2	June 4
B	Podium loosely surrounded by student hostel at university	B	Sept 15
C	Courtyard enclosed by student hostel at university	C	Sept 25
D	Open areas surrounded by commercial buildings	D1, D2, D3	Oct 16
E	Podium between teaching and office building at university	E1, E2, E3, E4	Nov 18
F	Podium enclosed by Public Housing buildings	F1, F2, F3, F4	Nov 19

short-wave radiant fluxes WSumK ($R^2 = 0.9986$) in Fig. 4b. Both relations are strongly and positively correlated with coefficient of determination R^2 which are nearly unity. The result shows that LMRT is strongly associated with the effective long-wave fluxes

emitted by the surrounding due to their surface temperatures. It is therefore LMRT could be an indicator of effective surface temperatures of surrounding objects in open spaces. This confirms the reason for the stronger correlation between LMRT and MRT under

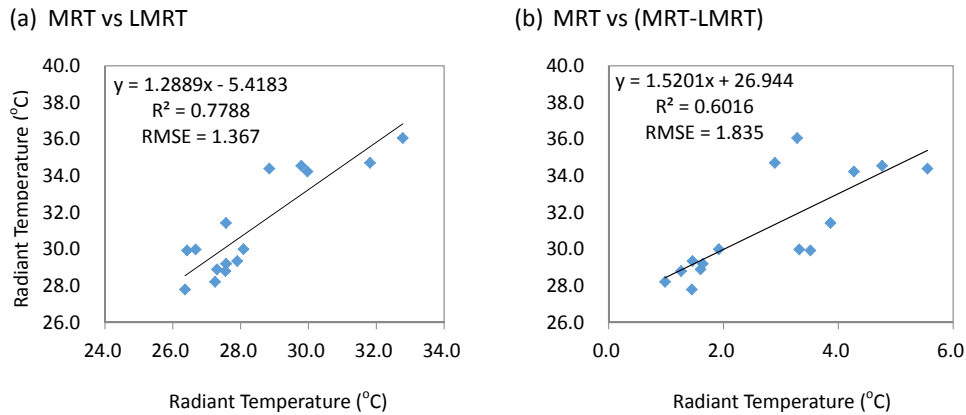


Fig. 3. Scatter plots for MRT.

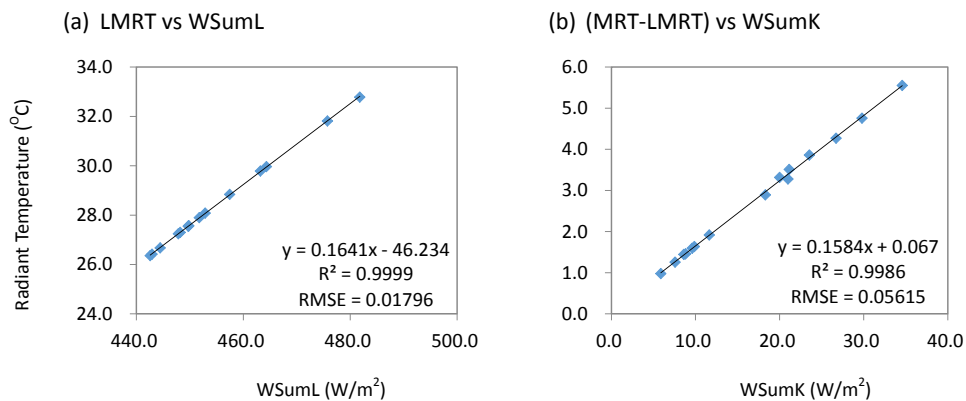


Fig. 4. Scatter plots for LMRT and (MRT – LMRT) against radiant fluxes.

shaded area. The higher the effective surface temperatures of surrounding, the higher LMRT, and the higher MRT. Also, the difference, (MRT-LMRT), could be an indicator of the effective sum of short-wave fluxes reflected by the surrounding and scattered by the sky. The larger the difference, the larger amount of short-wave fluxes that ‘trapped’ in open space.

The results suggest that mean radiant temperature MRT could be regressed on WSumL and WSumK simultaneously so as to evaluate how much MRT is increased for increase in either WSumL or WSumK. Multiple linear regression is thus performed for MRT on WSumL and WSumK. The equation is given by:

$$\text{MRT} = 0.1591 \text{ WSumL} + 0.1616 \text{ WSumK} - 43.96, R_a^2 \text{ of } 0.9999 \quad (5)$$

Based on regression analysis, the linear model is highly significant ($p < 0.001$, $N = 15$) with the adjusted R^2 of 0.9999, which is nearly unity. The RMSE is 0.02067. With the model, if WSumL in the environment is increased by 10 W/m^2 , the MRT would be estimated to increase by around 1.6 K with holding WSumK constant. Meanwhile, if WSumK in the environment is increased by 10 W/m^2 , the MRT would increase by around 1.6 K with holding WSumL constant. In other words, an increment of 1 K in MRT will be attributed to an increase of 6.25 W/m^2 in either WSumL or WSumK of the open spaces. The long-wave and short-wave fluxes existing in the outdoor spaces might be partly and jointly attributed to the climatic conditions or urban morphology.

3.3. Correlation between thermal indices and climatic conditions

The regression model of MRT on WSumL and WSumK shows that long-wave and short-wave fluxes have nearly equal influence on the increase in MRT. This might be because the placements of WSumL and WSumK are interchangeable in using defining equation of MRT by the *integral radiation method*. But, the above results also show LMRT, calculated only from WSumL, has a higher explanatory power for the variation in MRT. Because the relation between MRT and LMRT is more closely associated under shaded area than that between MRT and (MRT-LMRT). These lead to a question whether LMRT is not only correlated to the effective surface temperature of surrounding, but also associated with the ambient short-wave fluxes under climatic conditions of given global solar radiation and air temperature.

3.4. Correlation between thermal indices and reference air temperature

This session examined the association between thermal indices (MRT or LMRT) and a reference air temperature T_o , extracted from a Manned Weather Station ($22^\circ 18' 07'' \text{N}$, $114^\circ 10' 27'' \text{E}$) of Hong Kong Observatory. This weather station is located roughly at the centre of Hong Kong. The reference air temperature is thus used to represent one of the climatic conditions at the time of measurement. Fig. 5 shows the correlation between MRT/LMRT and T_o in shaded area under sunny conditions across different outdoor spaces. Both indices, MRT and LMRT, are positively and highly correlated with the reference air temperature with the coefficient of determination

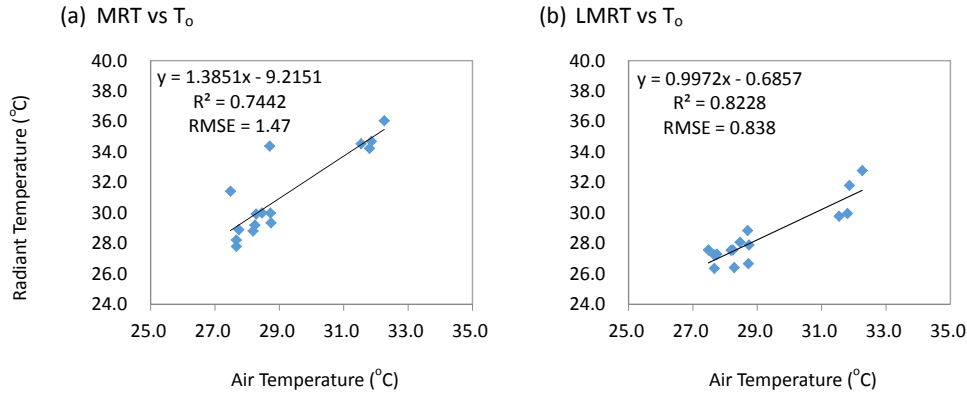


Fig. 5. Scatter plots for MRT and LMRT against reference air temperature.

R^2 of 0.74, and 0.82, respectively. The higher the T_o , the higher the LMRT and thus the higher MRT.

The reference air temperature, as an indicator of the regional air temperature, explained respectively 74%, and 82% of variations in MRT and LMRT. In other words, the local radiant temperature can be statistically and largely attributed to the variations in reference air temperature. This might imply that the local radiant temperature, especially the LMRT representing the local long-wave radiant fluxes of the open space between buildings, is largely mixed with the regional air temperature from radiative energy transfer perspective. But, there is still a moderate portion, around 20–25%, of variation in local radiant temperatures that cannot be explained by the reference air temperature. This unexplained part of MRT or LMRT might be attributed to other urban microclimatic factors due to the building neighbourhood, for example, the disposition and organization of buildings, the material of surrounding and so on. Nonetheless, the reference air temperature can provide a basic understanding of localized MRT (or LMRT when concerning about only long-wave component).

3.5. Correlation between thermal indices and global solar radiation

To further investigate the effect of climatic conditions on the thermal indices, we also examined the correlation between MRT/LMRT and the global solar radiation K_g , which extracted from the Kau Sai Chau (KSC) Automatic Weather Station (22°22'13"N, 114°18'45"E) of Hong Kong Observatory. Fig. 6 displays the scatter plots of MRT/LMRT against K_g in shaded area under sunny conditions in different outdoor spaces. The two thermal indices, MRT and LMRT, are also positively and highly correlated with the global solar radiation given at the time of measurement with coefficient of

determination R^2 of 0.85, and 0.71.

Regardless of air temperature, the global solar radiation also has a high explanatory power for both MRT and LMRT. The higher the global solar radiation, the higher the LMRT, and in turn the higher MRT. The global solar radiation is the driving force for heating up the air, and ambient objects around outdoor spaces resulting in higher ambient and surface temperatures of outdoor spaces, i.e. higher LMRT. This might explain the strong correlation between MRT/LMRT and global solar radiation. Also, with higher global solar radiation, it is more likely a larger amount of reflected solar radiation bouncing back from given building surfaces or other surfaces to the pedestrian level of outdoor spaces, and thus giving higher MRT. The result shows there is a high dependence of MRT/LMRT on global solar radiation at the time of measurement.

3.6. Correlation between radiant fluxes and climatic conditions

3.6.1. Correlation between radiant fluxes and reference air temperature

To scrutinize the effect of climatic conditions on mean radiant temperature, we also examined the correlation between WSumK/WSumL and reference air temperature T_o . Fig. 7a and b showed the dependence of WSumL and WSumK on reference air temperature. The WSumL is strongly correlated to the reference air temperature with R^2 of 0.82. This correlation is as strong as that between LMRT and reference air temperature T_o ($R^2 = 0.82$ as in Fig. 3b). Both correlations are stronger than that between MRT and T_o ($R^2 = 0.74$ in Fig. 5a). For another thing, the weighted sum of short-wave fluxes WSumK is weakly correlated to the reference air temperature with $R^2 = 0.25$. These show WSumL or LMRT are more correlated to reference air temperature than MRT because its short-wave

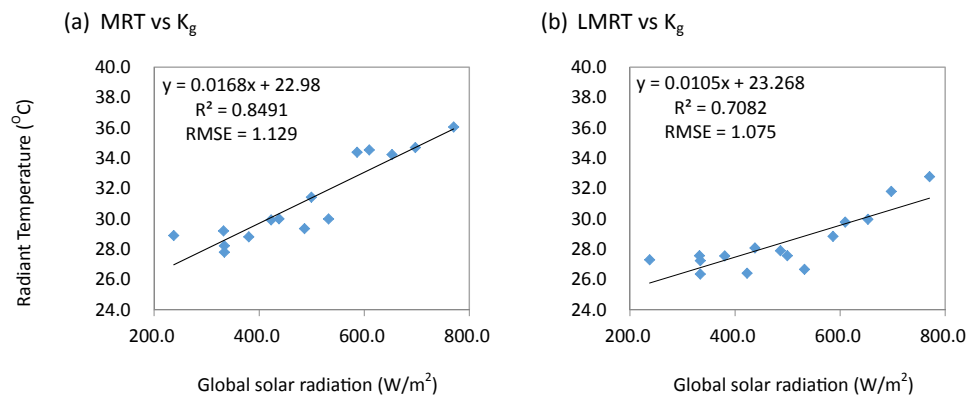


Fig. 6. Scatter plots for MRT and LMRT against global solar radiation.

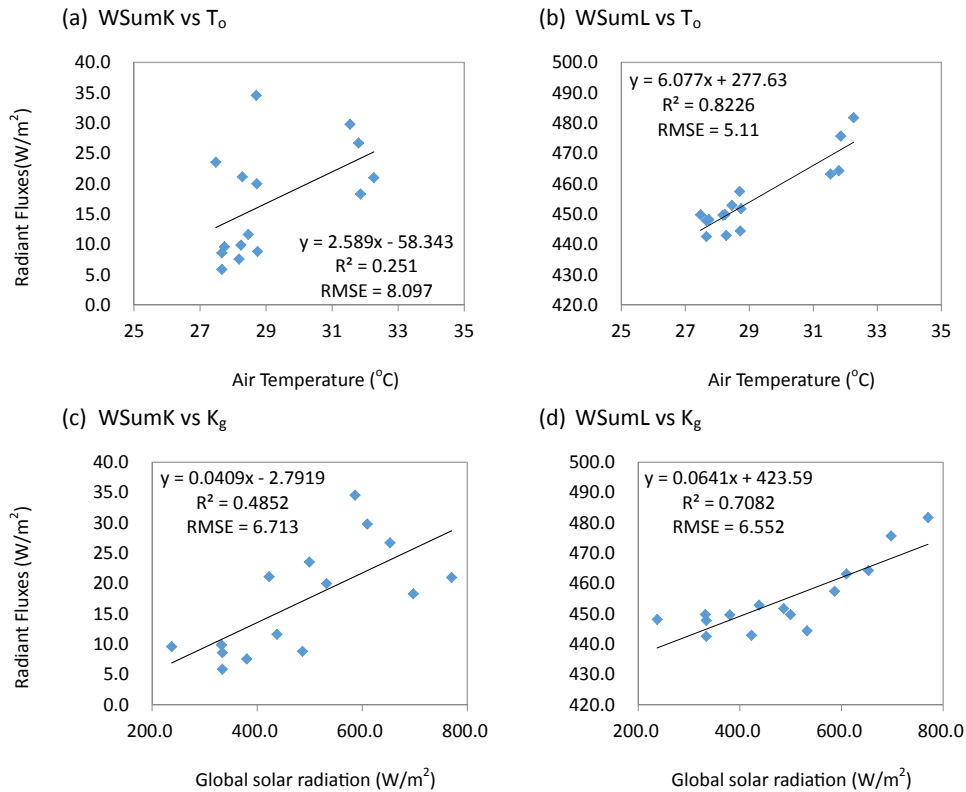


Fig. 7. Scatter plots for radiant fluxes against climatic factors.

components WSumK, barely correlated to, weaken the correlation between MRT and T_o . In short, the reference air temperature fundamentally effects the localized long-wave fluxes existing in open spaces. And the resulting long-wave fluxes provide the ground for mean radiant temperature.

3.6.2. Correlation between radiant fluxes and global solar radiation

For the effect of global solar radiation on WSumK and WSumL, Fig. 7c and d illustrate the correlations between global solar radiation K_g , and either WSumK or WSumL. Surprisingly, WSumK is not that strongly correlated to the K_g with R^2 of only 0.49. But, WSumL is strongly correlated to the global solar radiation K_g with $R^2 = 0.71$. This shows that the global solar radiation has impact on heating up the surfaces of surrounding objects resulting in emitting more long-wave fluxes as the surfaces are of higher surface temperature. For an increase of 100 W/m^2 in global solar radiation, the WSumL would be estimated to increase by 6.41 W/m^2 from Fig. 7d. This might bring an increase of slightly more than 1 K in MRT as aforementioned. On the other hand, an increase of 100 W/m^2 in global solar radiation would bring an increase of less than 1 K in MRT via the increase of WSumK. The above results suggest, when under shaded area, the LMRT or WSumL is playing a more important role in MRT. Controlling the amount of WSumL, and in turn LMRT, is more effective in achieving the desirable MRT when under shaded. Since the climatic conditions is hardly changed, like the global solar radiation and air temperature, the amount of WSumL might be easily adjusted when urban morphology is properly considered.

3.7. Correlation between radiant fluxes and SVF - case study

A case study was selected to scrutinize the effect of urban morphology on radiant fluxes on sunny day. Field measurements

were performed on June 4, 2015 by using net radiometers to record three-dimensional short-wave, long-wave fluxes and mean radiant temperature (Kipp & Zonen, CNR4) in an open space simultaneously at two measurement spots (Fig. 8): spot A1 was at the western part of the open space near to a skyscraper with curtain wall; spot A2 was located at the eastern area of the open space surrounded by several residential concrete buildings. The urban morphology around the open space is heterogeneous. Therefore, the Sky View Factor, SVF was employed to represent the complex urban structure. To capture the View Factor from the sensors perspective, fisheye photographs were taken in adjacent to each sensors of the radiometers. Not only the traditional SVF images were taken with fisheye lens facing upward for capturing Downward photons of visible light, namely SVF_{Downward} , but also the horizontal SVF (HSVF) images were taken for recording cardinal radiant fluxes: namely, Easterly (SVF_{Easterly}), Southerly ($SVF_{\text{Southerly}}$), Westerly (SVF_{Westerly}), and Northerly ($SVF_{\text{Northerly}}$). The fisheye photographs for Upward fluxes (SVF_{Upward}) were also taken but not in use in this study as the images were viewing the ground meaning no Sky View Factor could be recorded to represent the urban morphology. Only with sky views, the radiant fluxes (D, E, S, W, and N) is therefore correlated to the corresponding SVF (shown in Table 2) in order to examine the dependence of radiant fluxes on urban morphology.

3.7.1. Temporal pattern of LMRT and MRT

The long-wave mean radiant temperature LMRT for the two spots during the period 15:00–16:00 are shown in Fig. 9. The results showed that LMRT (blue lines) at spot A1 was also lower than that at spot A2 by 1 K in Fig. 9. $LMRT_{A1}$ was around 32°C , while $LMRT_B$ was around 33°C . This difference of 1 K might be attributed to the effect of immediate urban morphology on long-wave radiant fluxes. Also, both LMRT generally were quite steady and followed

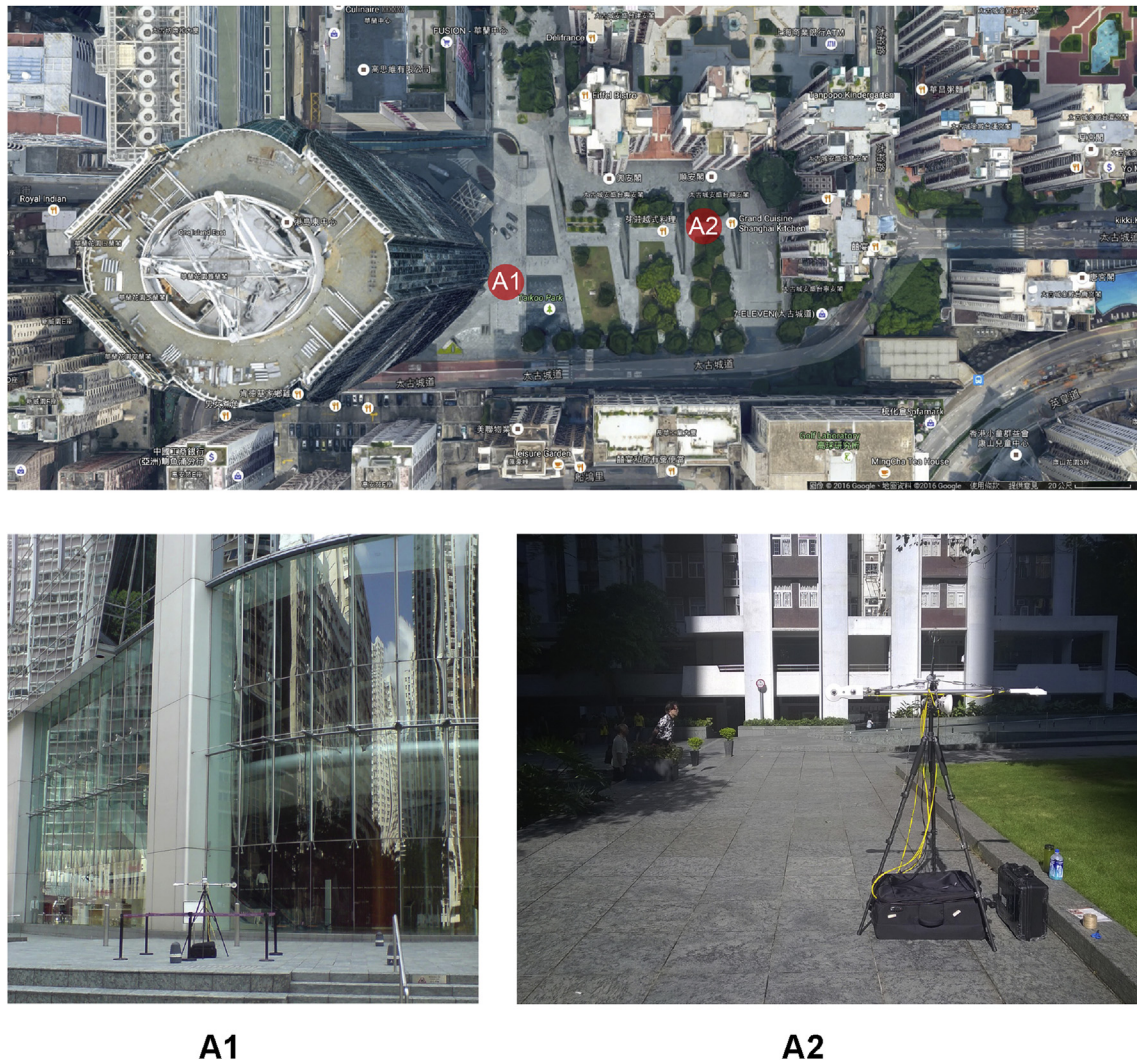


Fig. 8. Sites photos for the site A: spot A1 and A2.

the temporal pattern of the reference air temperature T_0 (purple line) recorded by the Hong Kong Observatory for different sites during the period 15:00–16:00. These also showed the strong correlation between LMRT and T_0 , and justified the introduction of LMRT as a thermal index for effective surface temperature of surrounding instead reference air temperature.

The mean radiant temperature MRT for the two spots during the period 15:00–16:00 are shown in Fig. 9. The MRT (red line) at spot A1 was lower than that at spot A2 during that period. At spot A1, the measured MRT_{A1} , was around or below 35 °C. But, at spot A2, the measured MRT_{A2} , was between 36 and 39 °C from 15:00–15:45, and since then it was rising up to around 55 °C from 15:45–16:00. The large difference in MRT between spot A1 and A2 was due to the latter spot receiving larger amount of short-wave fluxes: more diffuse and reflected fluxes during 15:00–15:45; more beam solar radiation from 15:45–16:00 at the time of low angle sun. Without shading, spot A2 experienced a sudden large increase in MRT from around 40 to 55 °C at 15:45 due to direct solar radiation. With shading during 15:00–15:45, spot A1 still experienced a higher MRT due to urban morphology.

Both LMRT and MRT were lower at spot A1 than at spot A2. The ambient long-wave fluxes were less at spot A1; at the same time ambient short-wave fluxes were more at spot A2. The differences in LMRT or MRT were attributed to the ambient radiant fluxes at the

spots. This led to a question how, to what extent, the ambient urban morphology affect the local radiant fluxes.

3.7.2. Relationship between long-wave radiant fluxes and SVF

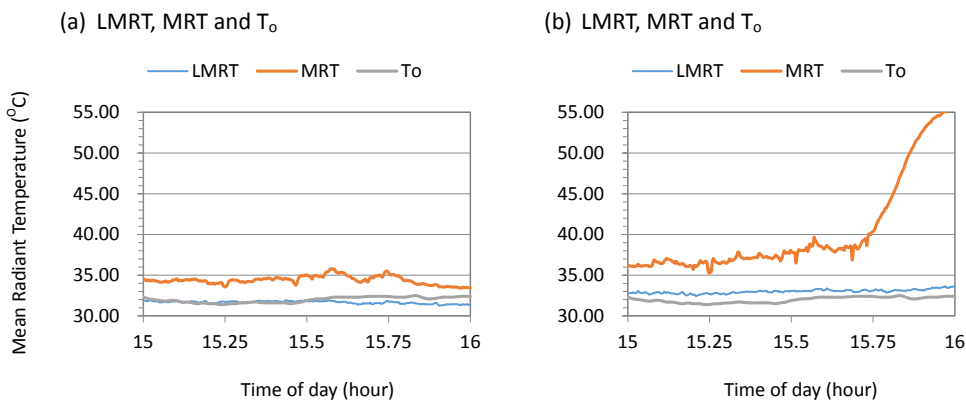
For the long-wave fluxes at both spots, the upward one were the highest, but the downward one were the least. While the amount of cardinal fluxes were between the upward and downward ranging from 480 to 510 W/m^2 for most of the time. At both spot A1 and A2, the upward long-wave fluxes from the ground were steady and around 510 W/m^2 during 15:00–16:00 because both spots had the same pavement.

There was seemingly an effect of SVF on amount of long-wave fluxes: the larger the sky views, the larger the cooling rate, and the less long-wave fluxes from the sky. For example, in Fig. 10a) and b), the downward long-wave fluxes at spot A1 $L_{Downward, A1}$ was lower than that at spot A2 by around 20 W/m^2 where $SVF_{Downward, A1}$ was 0.242; $SVF_{Downward, A2}$ was 0.185. $L_{Downward, A1}$ was between 458 and 464 W/m^2 ; but $L_{Downward, A2}$ was between 476 and 482 W/m^2 . Another example was that the Northerly fluxes at spot A1 was lower than at spot A2 by around 15 W/m^2 with $SVF_{Northerly, A1}$ was 0.126; $SVF_{Northerly, A2}$ was 0.086. $L_{Northerly, A1}$ was between 484 and 486 W/m^2 ; but the $L_{Northerly, A2}$ was larger than 502 W/m^2 . Third, the Southerly fluxes at spot A1 was slightly lower than at spot A2. $L_{Southerly, A1}$ was around 488–490 W/m^2 with $SVF_{Southerly, A1}$

Table 2

Summary of Sky View Factor values from five directions: D, N, S, W, and E for measurement at spot A1 and A2.

Direction	Spot A1	Spot A2
Downward D	 0.242	 0.185
Northerly N	 0.126	 0.086
Southerly S	 0.147	 0.138
Westerly W	 0.098	 0.137
Easterly E	 0.191	 0.108

**Fig. 9.** Temporal profile of MRT for Spot A1 and A2 during 15:00–16:00.

$A1 = 0.147$; $SVF_{\text{Southerly}, A2} = 0.138$. $L_{\text{Southerly}, A2}$, was slight larger than 490 W/m^2 , but less than 494 W/m^2 . The fourth example was that the Westerly fluxes at spot A1 was larger than at spot A2 by at least $2\text{--}4 \text{ W/m}^2$ during 15:00–15:45 where $SVF_{\text{Westerly}, A1} = 0.098$; $SVF_{\text{Westerly}, A2} = 0.137$. $L_{\text{Westerly}, A1}$, was between 496 and 498 W/m^2 ; but $L_{\text{Westerly}, A2}$, was around 494 W/m^2 . After 15:45, $L_{\text{Westerly}, A2}$, was rising due to beam solar radiation when the sun at low angle and becoming larger than $L_{\text{Westerly}, A1}$. One exemption was that the Easterly fluxes at spot A1 was less than at spot A2 by at least 10 W/m^2 during 15:00–16:00 where $SVF_{\text{Easterly}, A1} = 0.191$; $SVF_{\text{Easterly},$

$A2 = 0.108$. $L_{\text{Easterly}, A1}$, was around $488\text{--}490 \text{ W/m}^2$; $L_{\text{Easterly}, A2}$, was larger than 500 W/m^2 . It was because of the beam solar radiation was incident on west-facing building facades near spot A2 resulting in higher surface temperature and larger amount of easterly long-wave fluxes. The above results generally showed that more SVF, less long-wave radiant fluxes. Moreover, the larger the difference in SVF, the larger the difference in long-wave radiant fluxes. Exemption was found if there were more sunlit area besides the SVF.

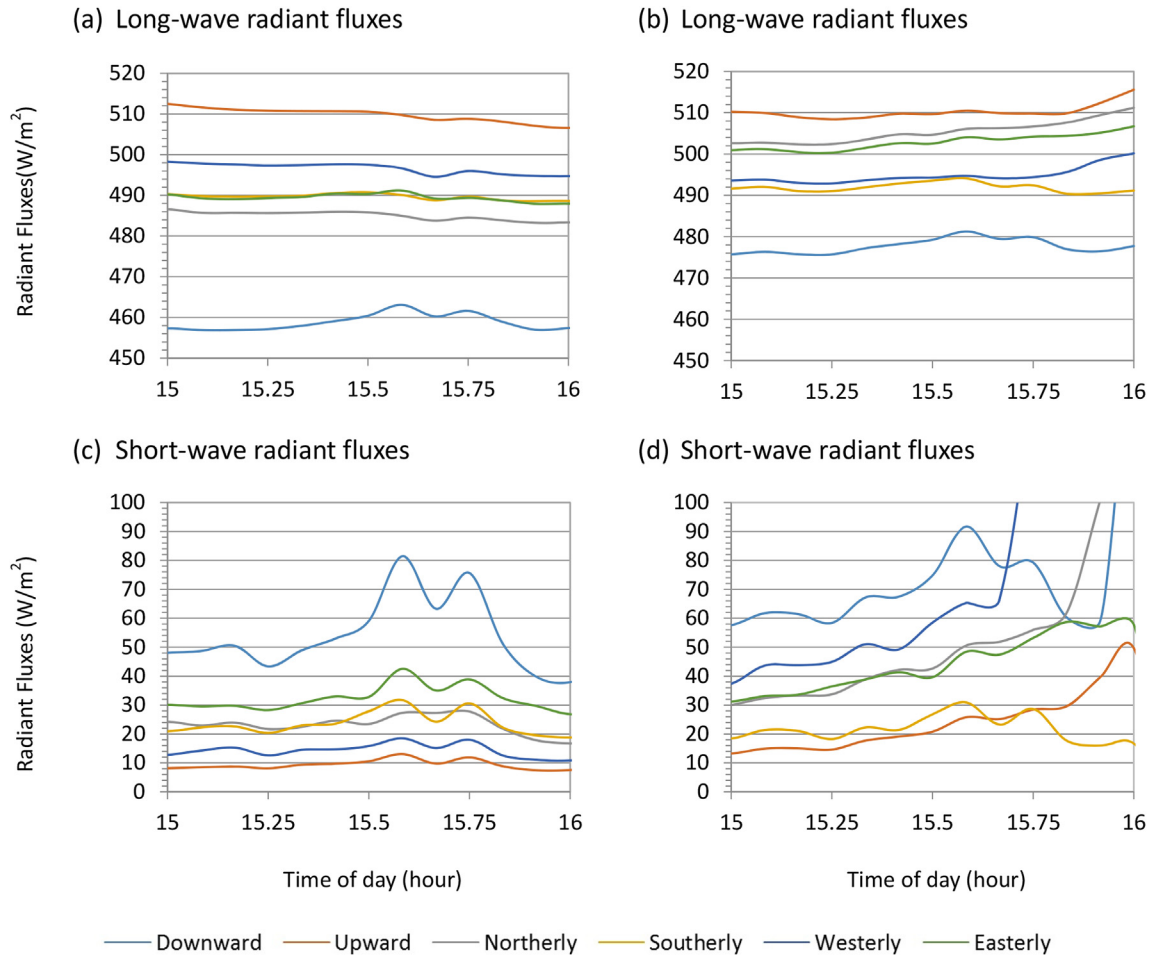


Fig. 10. Temporal profile of radiant fluxes for Spot A1 and A2 in 15:00–16:00.

3.7.3. Relationship between short-wave radiant fluxes and SVF

For the short-wave fluxes at both spots, the downward one generally were the highest, but the upward one were the least when no beam solar radiation incident on the sensors during 15:00–15:45. While the amount of cardinal fluxes were between the downward and upward one for most of the time except for 15:45–16:00 at the time of low angle sun.

In general, all short-wave radiant fluxes at spot A1 were lower than that at spot A2 for each corresponding direction as shown in Fig. 10c) and d). For spot A1, the short-wave fluxes from the five directions were all steady and below 100 W/m² as spot A1 was in the shade of a skyscraper at its western side blocking the sun. But, for spot A2, the short-wave fluxes from all directions were all steadily increasing as this spot was more open to the western sky allowing more diffuse and beam solar radiation reaching it. To examine the effect of SVF on short-wave radiant fluxes at the two spots, it is worth noting the directional fluxes as follows:

First, the Southerly fluxes at spot A1, $K_{\text{Southerly}, A1}$, was nearly the same as that at spot A2 $K_{\text{Southerly}, A2}$ during 15:00–16:00. Because both spots faced similar building cluster at their south with similar SVF ($SVF_{\text{Southerly}, A1} = 0.147$; $SVF_{\text{Southerly}, A2} = 0.138$), their southerly fluxes followed the same temporal pattern, and thus ranged from 20 to 30 W/m². Second, the Westerly fluxes at A2 was much higher than that at A1 by at least 30 W/m². The westerly fluxes at A1 was quite steady between 10 and 20 W/m² as spot A1 was in the shade of a skyscraper ($SVF_{\text{Westerly}, A1} = 0.098$). But westerly fluxes at spot A2 increased steadily before 15:40 due to increasing diffuse sky

radiation as the sensor faced the west where sunset was about to happen. After 15:40, the westerly fluxes at A2 increased sharply as beam solar radiation from low angle sun was directly incident on the west-facing sensor ($SVF_{\text{Westerly}, A2} = 0.137$). Third, the Northerly and Easterly fluxes at A2 was larger than that at A1 by a smaller differences of less than 30 W/m². Though the SVFs at A2 were smaller than that at A1 ($SVF_{\text{Northerly}, A1} = 0.126 > SVF_{\text{Northerly}, A2} = 0.086$; $SVF_{\text{Easterly}, A1} = 0.191 > SVF_{\text{Easterly}, A2} = 0.108$). The higher values of short-wave fluxes at A2, especially for the easterly fluxes, might be due to more reflected solar radiation bouncing back from the west-facing wall when the sun was at low angle. Also, the downward short-wave fluxes at spot A1 $K_{\text{Downward}, A1}$, was lower than that at spot A2 by around 20 W/m² where $SVF_{\text{Downward}, A1} = 0.242$ and $SVF_{\text{Downward}, A2} = 0.185$.

It is therefore not obvious to conclude a simple dependence of short-wave fluxes on SVF when under shaded, which as manifestation of urban morphology. This case study showed that the existing short-wave fluxes not only depended on the amount of visible area of the sky views, but also depended on the relative position of sun, and relative disposition and orientation of building façade.

3.7.4. Correlation between SVF and radiant fluxes

This case study investigated the dependence of radiant fluxes on the SVF as indicator of urban morphology. Fig. 11 showed the correlation between SVF and radiant fluxes under shaded area as in Fig. 11 a) and c); and unshaded as in Fig. 11 b) and d), in a sunny day.

The higher SVF, the less long-wave radiant fluxes; and the slightly more short-wave fluxes when under shaded. For instance, when the sensors at both spots under shaded at 15:00 as in Fig. 11 a) and c), the directional long-wave fluxes is strongly correlated to the directional SVF with R^2 of 0.81. But, the directional short-wave fluxes is barely correlated to the directional SVF with R^2 of 0.40. The Sky View Factor has a high explanatory power for the long-wave fluxes; and only moderate one for short-wave fluxes under shaded conditions.

The higher SVF, the less long-wave radiant fluxes; but no clear dependence of short-wave fluxes on SVF in unshaded area. For example, when the sensor was not under shaded at 15:45 as in Fig. 11 b) and d), the directional long-wave fluxes is still strongly correlated to the directional SVF with R^2 of 0.79, while the directional short-wave fluxes is not correlated to SVF. The Sky View Factor still has a higher explanatory power for the long-wave fluxes, but not for the short-wave fluxes when involved unshaded spot.

These showed a strong effect of SVF on long-wave fluxes, and in turn the weighted sum of long-wave fluxes, WSumL: higher SVF, less long-wave fluxes. If directional SVF in the environment is increased by 0.1, the directional long-wave fluxes would be estimated to decrease by at least 20 W/m² with holding other factors constant. For example, if SVF_{Northerly} is increased by 0.1, then L_{Northerly} would be decreased, to be conservative, by 20 W/m². Moreover, if SVF is increased by 0.1, for example, at the north-eastern side of the sky dome, then SVF_{Northerly}, SVF_{Easterly} and SVF_{Downward} would be increased by 0.1 at the same time, and therefore L_{Northerly}, L_{Easterly}, and L_{Downward} would be simultaneously decreased by 20 W/m². These result in a total decrease of $(0.22 + 0.22 + 0.06) \cdot 20 \text{ W/m}^2 = 10 \text{ W/m}^2$ in WSumL if SVF is increased by 0.1 as for a standing

person the weighting is 0.22 for each horizontal fluxes, and is 0.06 for downward fluxes. In other words, if SVF of the sky dome is increased by 0.1, the WSumL would be decreased by around 10 W/m².

4. Conclusions

Across different open spaces and climatic conditions in Hong Kong, if WSumL in the environment is increased by 10 W/m², the MRT would be estimated to increase by around 1.6 K with holding WSumK constant. Meanwhile, if WSumK in the environment is increased by 10 W/m², the MRT would increase by around 1.6 K with holding WSumL constant.

The study also reveals the strong correlation between radiant fluxes and climatic conditions of given global solar radiation and daily reference air temperature. LMRT, is positively and highly correlated with the reference air temperature. The regional reference air temperature fundamentally effects the localized long-wave fluxes existing in open spaces. And the resulting long-wave fluxes provide the ground, i. e, LMRT, for mean radiant temperature. In additions, for an increase of 100 W/m² in global solar radiation, the WSumL would be estimated to increase by 6.41 W/m². This might bring an increase of slightly more than 1 K in MRT. The same increase in global solar radiation would bring an increase of less than 1 K in MRT via the increase of WSumK. These two climatic factors are the most influential meteorological parameters affecting the long-wave and short-wave radiant fluxes components in MRT.

Under the same climatic condition, a case study shows that the variations in long-wave and short-wave radiant fluxes are also attributed to the Sky View Factor of the densely built environment.

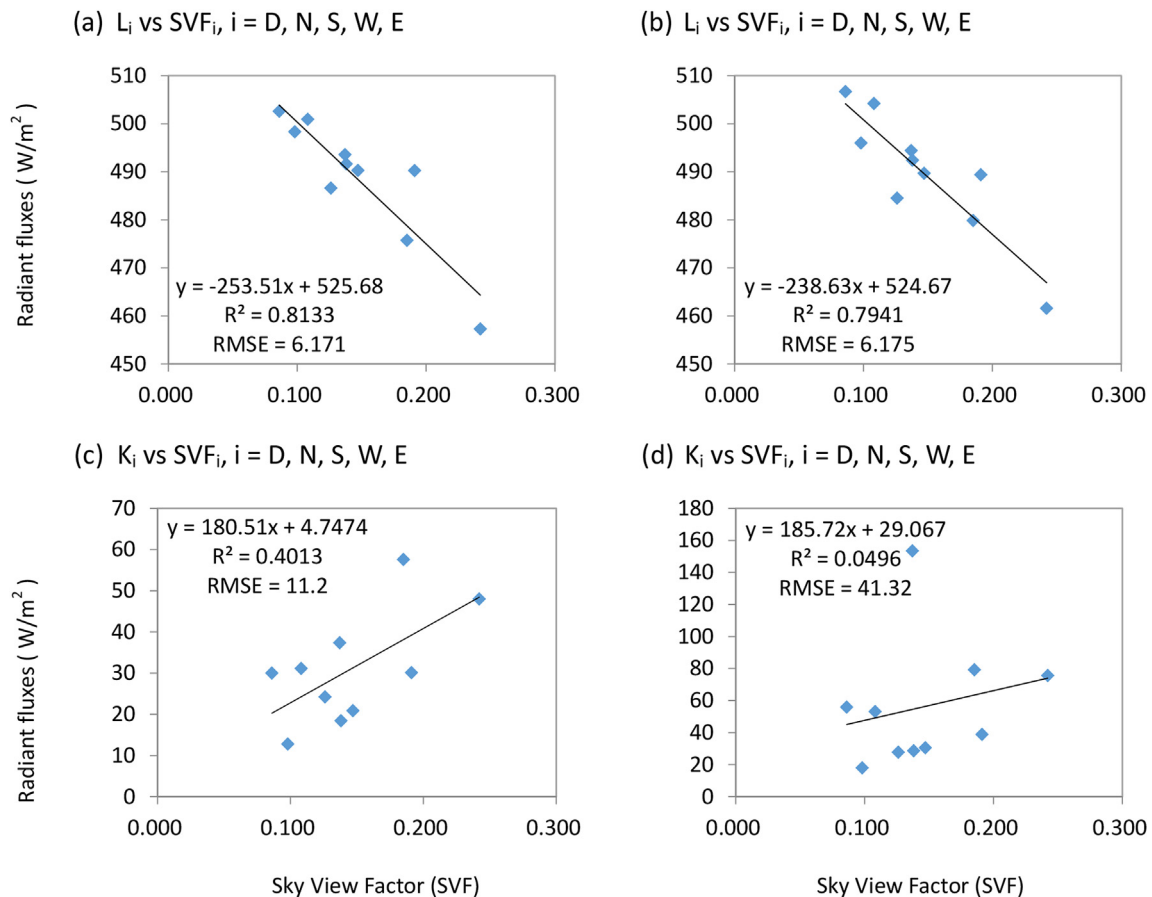


Fig. 11. Scatter plots of radiant fluxes against SVF for Site A un/der shaded.

The sky view, SVF is significantly correlated to radiant fluxes: short-wave fluxes with weakly positive association; but long-wave fluxes with stronger and negative one. The lower SVF, the more long-wave radiant fluxes either under shaded or unshaded. If SVF of the sky dome is decreased by 0.1, the WSumL would be increased by around 10 W/m². This would bring an increase of 1.6 K in MRT. These shows indirectly the effect of urban morphology, represented by SVF, on MRT via its component radiant fluxes, especially the long-wave fluxes.

5. Implications for design strategies in open space

This study has revealed the effect of SVF as cooling strategy in addition to its shading effect. The results have taken a step in the direction of refining the urban design strategies to minimize the negative aspects of site layout relating to microclimate to the neighbouring buildings and public areas as outlined in section SA 4 Site Design Appraisal of BEAM Plus for New Building Version 1.2 [35].

To design a comfortable open spaces for people to live healthily in the densely built environment, strategic disposition of buildings is crucial for effective shading of outdoor space to block the direct short-wave from the sun, and, for effective cooling of open space to loss sensible heat that being trapped between buildings:

- Shading could be provided to the open space by suitable disposition of building envelopes to minimize the prolonged exposure of direct solar radiation in hot and/or humid seasons, particularly in the afternoon session;
- Appropriate disposition of building envelopes could help the radiative cooling of open spaces, and avoid radiative heating of them;
- Together with the first point, adequately wide gaps should be provided between building envelopes to maximize the sky view for better cooling effect of open spaces. The gaps for enhancing the cooling effect should be provided to be viewed at pedestrian level within the open spaces.

Acknowledgements

The authors would like to thank the Construction Industry Council (CIC) of Hong Kong for financially supporting this research under the research project (Project ID: CICR/04/13): 'A Study of Impact of Building Envelope on Urban Outdoor Thermal Environment'. The authors are also thankful to Mr. Julian Lee and Ms. Judy Zhang for their effort and kind help and cordially thank Mr. Max Lee for setting up the equipment. Last but not least, special thanks to all the property officers of the relevant open spaces for the permission of field measurement and their kind support.

References

- [1] T.P. Lin, A. Matzarakis, R.L. Hwang, Shading effect on long-term outdoor thermal comfort, *Build. Environ.* 45 (2010) 213–221.
- [2] T.P. Lin, K.T. Tsai, R.L. Hwang, A. Matzarakis, Quantification of the effect of thermal indices and sky view factor on park attendance, *Landsc. Urban Plan.* 107 (2012) 137–146.
- [3] A.A. Hakim, H. Petrovitch, C.M. Burchfiel, G.W. Ross, B.L. Rodriguez, L.R. White, Effects of walking on mortality among non-smoking retired men, *N. Engl. J. Med.* 338 (1998), 94–9.
- [4] C.L. Tan, N.H. Wong, S.K. Jusuf, Outdoor mean radiant temperature estimation in the tropical urban environment, *Build. Environ.* 64 (2013) 118–129.
- [5] P.O. Fanger, *Thermal comfort*, McGraw-Hill, New York, 1972.
- [6] Y. Epstein, D.S. Moran, Thermal comfort and the heat stress indices, *Ind. Health* 44 (3) (2006) 388–398.
- [7] K.C. Parsons, *Human Thermal Environments: the Effects of Hot, Moderate, and Cold Environments on Human Health, Comfort and Performance*, Taylor & Francis, London, New York, 2003.
- [8] ASHRAE, *ASHRAE Fundamentals Handbook 2013 (SI Edition)*, American Society of Heating, Refrigerating, and Air-Conditioning Engineers, 2013. ISBN: 978-1936504466.
- [9] P. Höppe, The physiological equivalence temperature – a universal index for the biometeorological assessment of the thermal environment, *Int. J. Biometeorol.* 43 (2) (1999) 71–75.
- [10] G. Jendritzky, R. de DEAR, G. Havenith, UTCI – why another thermal index? *Int. J. Biometeorol.* 56 (2012) 421–428.
- [11] N. Walikewitz, B. Janicke, M. Langner, F. Meier, W. Endlicher, The difference between the mean radiant temperature and the air temperature within indoor environments: a case study during summer conditions, *Build. Environ.* 84 (2015) 151–161.
- [12] A. Matzarakis, B. Amelung, Physiological equivalent temperature as indicator for impacts of climate change on thermal comfort of humans, in: M. Thomson, R. Garcia-Herrera, M. Beniston (Eds.), *Seasonal Forecasts, Climatic Change and Human Health*, Springer, Netherlands, 2008, pp. 161–172.
- [13] N. Kántor, J. Unger, The most problematic variable in the course of human-biometeorological comfort assessment – the mean radiant temperature, *Centeurjgeo* 3 (2011) 90–100.
- [14] M. Langner, K. Scherber, W. Endlicher, Indoor heat stress: an assessment of human bioclimate using the UTCI in different buildings in Berlin, *Die Erde* 144 (2013) 260–273.
- [15] D. Pearlmutter, A. Bitan, P. Berliner, Microclimatic analysis of "compact" urban canyons in an arid zone, *Atmos. Environ.* 33 (24–25) (October 1999) 4143–4150.
- [16] F. Bouria, H.B. Awbi, Building cluster and shading in urban canyon for hot dry climate Part 1: air and surface temperature measurements, *Renew. Energy* 29 (2004) 249–262.
- [17] E. Johansson, Influence of urban geometry on outdoor thermal comfort in a hot dry climate: a study in Fez, Morocco, *Build. Environ.* 41 (2006) 1326–1338.
- [18] R. Hamdi, G. Schayes, Sensitivity study of the urban heat island intensity to urban characteristics, *Int. J. Climatol.* 28 (2007) 973–982.
- [19] E.L. Krüger, F.O. Minella, F. Rasia, Impact of urban geometry on outdoor thermal comfort and air quality from field measurements in Curitiba, Brazil, *Build. Environ.* 46 (2011) 621–634.
- [20] E. Jamei, P. Rajagopalan, M. Seyedmahmoudian, Y. Jamei, Review on the impact of urban geometry and pedestrian level greening on outdoor thermal comfort, *Renew. Sustain. Energy Rev.* 54 (2016) 1002–1017.
- [21] S. Watanabe, K. Nagano, J. Ishii, T. Horikoshi, Evaluation of outdoor thermal comfort in sunlight, building shade, and pergola shade during summer in a humid subtropical region, *Build. Environ.* 82 (2014) 556–565.
- [22] E. Andreou, Thermal comfort in outdoor spaces and urban canyon microclimate, *Renew. Energy* 55 (2013) 182–188.
- [23] S. Achour-Younsi, F. Kharrat, Outdoor thermal comfort: impact of the geometry of an urban street canyon in a Mediterranean subtropical climate – case study Tunisia, *Tunisia, Procedia – Soc. Behav. Sci.* 216 (2016) 689–700.
- [24] T.R. Oke, Street design and urban canopy layer climate, *Energy Build.* 11 (1988) 103–113.
- [25] J. Unger, Connection between urban heat island and sky view factor approximated by a software tool on a 3D urban database, *Int. J. Environ. Pollut.* 36 (Nos. 1/2/3) (2009) 59–80.
- [26] F. Ali-Toudert, H. Mayer, Numerical study on the effects of aspect ratio and orientation of an urban street canyon on outdoor thermal comfort in hot and dry climate, *Build. Environ.* 41 (2) (2006) 94–108.
- [27] H. Lee, J. Holst, H. Mayer, Modification of human-biometeorologically significant radiant flux densities by shading as local method to mitigate heat stress in summer within urban street canyons, *Adv. Meteorol.* (2013) 312572, <http://dx.doi.org/10.1155/2013/312572>.
- [28] H. Lee, H. Mayer, D. Schindler, Importance of 3-D radiant flux densities for outdoor thermal comfort on clear-sky summer days in Freiburg, Southwest Germany, *Meteorol. Z.* (2014), <http://dx.doi.org/10.1127/0941-2948/2014/0536>.
- [29] D. Pearlmutter, P. Berliner, E. Shaviv, Physical modelling of pedestrian energy exchange within urban canopy, *Build. Environ.* 41 (2006) 783–795.
- [30] F. Bourbia, F. Boucheriba, Impact of street design on urban microclimate for semi arid climate (Constantine), *Renew. Energy* 35 (2010) 343–347.
- [31] P. Weihs, H. Staiger, B. Tinz, E. Batchvarova, H. Rieder, L. Vuilleumier, et al., The uncertainty of UTCI due to uncertainties in the determination of radiation fluxes derived from measured and observed meteorological data, *Int. J. Biometeorol.* 56 (2012) 537–555.
- [32] S. Thorsson, F. Lindberg, I. Eliasson, B. Holmer, Different methods for estimating the mean radiant temperature in an outdoor urban setting, *Int. J. Climatol.* 27 (2007) 1983–1993.
- [33] VDI, *Environmental Meteorology, Interactions between Atmosphere and Surface; Calculation of Short- and Long-wave Radiation, Part I: Climate*, VDI 3789, Part: VDI/DIN – Handbuch Reinhaltung der Luft, Band 1b, Düsseldorf, 1994.
- [34] Kipp and Zonen CNR4 instruction manual. <http://www.kippzonen.com/Product/85/CNR4-Net-Radiometer#.WDj5z4VOI6Y> (accessed 25.11.2016).
- [35] HKGBC (Hong Kong Green Building Council Limited), BEAM Plus for New Building Version 1.2, 2012. https://www.hkgbc.org.hk/eng/BPRef-manuals_assessment.aspx, 2012 (accessed 25.11.2016).